



# Ultrafast spectroscopy tracks carotenoid configurations in the orange and red carotenoid proteins from cyanobacteria

Václav Šlouf<sup>1</sup> · Valentyna Kuznetsova<sup>1</sup> · Marcel Fuciman<sup>1</sup> · Céline Bourcier de Carbon<sup>2,3</sup> · Adjélé Wilson<sup>2,3</sup> · Diana Kirilovsky<sup>2,3</sup>  · Tomáš Polívka<sup>1,4</sup> 

Received: 7 May 2016 / Accepted: 30 August 2016 / Published online: 9 September 2016  
© Springer Science+Business Media Dordrecht 2016

**Abstract** A quenching mechanism mediated by the orange carotenoid protein (OCP) is one of the ways cyanobacteria protect themselves against photooxidative stress. Here, we present a femtosecond spectroscopic study comparing OCP and RCP (red carotenoid protein) samples binding different carotenoids. We confirmed significant changes in carotenoid configuration upon OCP activation reported by Leverenz et al. (Science 348:1463–1466. doi: [10.1126/science.aaa7234](https://doi.org/10.1126/science.aaa7234), 2015) by comparing the transient spectra of OCP and RCP. The most important marker of these changes was the magnitude of the transient signal associated with the carotenoid intramolecular charge-transfer (ICT) state. While OCP with canthaxanthin exhibited a weak ICT signal, it increased significantly for canthaxanthin bound to RCP. On the contrary, a strong ICT signal was recorded in OCP binding echinenone excited at the red edge of the absorption spectrum. Because the carbonyl

oxygen responsible for the appearance of the ICT signal is located at the end rings of both carotenoids, the magnitude of the ICT signal can be used to estimate the torsion angles of the end rings. Application of two different excitation wavelengths to study OCP demonstrated that the OCP sample contains two spectroscopically distinct populations, none of which is corresponding to the photoactivated product of OCP.

**Keywords** Orange carotenoid protein · Red carotenoid protein · Non-photochemical quenching · Intramolecular charge-transfer state · Ultrafast spectroscopy

## Introduction

Oxygen-dependent photosynthetic organisms such as plants, algae and cyanobacteria must protect themselves against photooxidative stress. Key players in this process are carotenoids. They quench both the reactive oxygen species such as singlet oxygen, but also prevent those species from being generated by quenching excited states of “parent” molecules, i.e., chlorophylls or phycobilins. When the parent molecules are in the singlet excited state, the process of their assisted deexcitation is called non-photochemical quenching (NPQ), which is manifested as a decrease in their fluorescence (Niyogi and Truong 2013).

Cyanobacteria utilize three specific types of NPQ: One is based on the iron stress-induced isiA protein (Yeremenko et al. 2004; Ihalainen et al. 2005), another operates in the recently described HliD protein, which is an ancestor of antennas from LHC superfamily (Staleva et al. 2015), and, finally, the last type of quenching is associated with the orange carotenoid protein (OCP), which is in the focus of this study. This water-soluble, carotenoid-binding

**Electronic supplementary material** The online version of this article (doi:[10.1007/s11120-016-0302-6](https://doi.org/10.1007/s11120-016-0302-6)) contains supplementary material, which is available to authorized users.

✉ Tomáš Polívka  
tpolivka@jcu.cz

<sup>1</sup> Institute of Physics and Biophysics, Faculty of Science, University of South Bohemia, Branišovská 1760, 370 05 České Budějovice, Czech Republic

<sup>2</sup> Institute for Integrative Biology of the Cell (I2BC), CEA, CNRS, Université Paris-Sud, Université Paris-Saclay, 91198 Gif-sur-Yvette, France

<sup>3</sup> Institut de Biologie et Technologies de Saclay (iBiTec-S), Commissariat à l’Energie Atomique (CEA), 91191 Gif-sur-Yvette, France

<sup>4</sup> Institute of Plant Molecular Biology, Biological Centre, Czech Academy of Sciences, Branišovská 31, 370 05 České Budějovice, Czech Republic

protein was first identified in 1981 (Holt and Krogmann 1981). It is responsible for quenching of phycobilisome fluorescence (Wilson et al. 2006; see also Kirilovsky 2007 for review). The crystal structure of the *Arthrospira maxima* OCP with the carotenoid 3'-hydroxyechinenone was resolved (2.1 Å) in 2003 (Kerfeld et al. 2003) and that of *Synechocystis* PCC6803 with echinenone (1.65 Å) in 2010 (Wilson et al. 2010). Only recently, another X-ray structure of OCP from *Synechocystis* PCC6803 (produced in *Escherichia coli*) binding the carotenoid canthaxanthin was obtained, with resolution of 1.9 Å (Leverenz et al. 2015).

OCP consists of two domains: an  $\alpha$ -helical N-terminal domain, which is unique to cyanobacteria, and an  $\alpha$ -helix/ $\beta$ -sheet C-terminal domain which is a member of the NTF2 (nuclear transport factor 2) superfamily that can be found in a wide range of organisms (Kerfeld et al. 2003; Wilson et al. 2010). The carotenoid spans both domains, thus contributing to stabilization of both parts of the protein. There are also other ways the overall protein conformation is stabilized: a flexible linker about 25 residues long between the C- and N-terminal domain; the first 19 amino acids of the N-terminal domain interacting with the surface of the C-terminal domain; a salt bridge between two charged amino acids, each located in another domain.

The relationship between the OCP presence/absence and phycobilisome fluorescence quenching induced by blue–green light was identified 10 years ago by mutational studies (Wilson et al. 2006). It was shown that fluorescence quenching was inhibited and the photoinhibition was faster in mutants lacking the OCP. Only later it was realized that OCP is a photoactive protein (Wilson et al. 2008). Upon illumination with blue–green light, it undergoes a transition from an inactive orange form (OCPo) to an active red form (OCP<sub>r</sub>), the latter being an effector in fluorescence quenching. Spectrally, the two forms of OCP not only differ in the redshift of OCP<sub>r</sub> with respect to OCPo, but the activation is also accompanied by the loss of carotenoid vibrational structure, suggesting diminished binding constraints of the carotenoid in OCP<sub>r</sub>.

OCP from *Synechocystis* is able to bind 3'-hydroxyechinenone, echinenone, canthaxanthin and zeaxanthin (Fig. 1). OCP with all the mentioned carotenoids except zeaxanthin can be activated by blue–green light (Punginelli et al. 2009; de Carbon et al. 2015). Consequently, no quenching is induced by OCP binding zeaxanthin (Punginelli et al. 2009). The presence of a carbonyl group is, thus, essential for the activation because zeaxanthin is a non-carbonyl carotenoid. The importance of the carbonyl group is supported by the fact that it forms a hydrogen bond to two neighboring residues, Tyr201 and Trp288 (Kerfeld et al. 2003; Wilson et al. 2010). When these residues were mutated, the specificity for binding the carbonyl carotenoid was

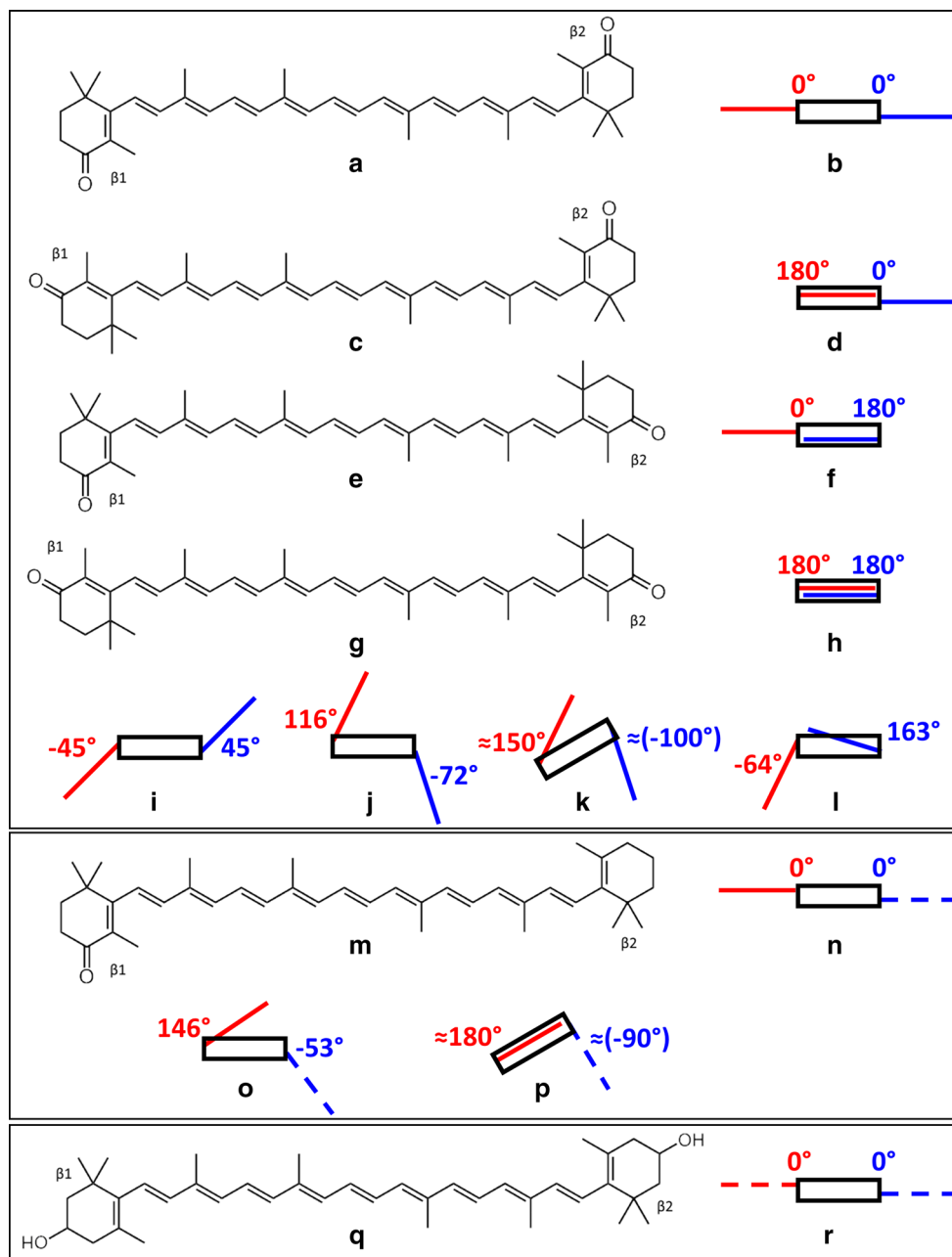
diminished. Additionally, neither photoactivation nor fluorescence quenching was observed in these mutants (Wilson et al. 2011).

Carbonyl carotenoids are known for their specific polarity-dependent behavior. Their spectroscopic properties in nonpolar solvents are comparable to their non-carbonyl counterparts. The excitation promotes the carotenoid from the ground state,  $S_0$ , to the second excited state,  $S_2$ . The carotenoid then relaxes to the first excited state,  $S_1$ , on the timescale of hundreds of femtoseconds. The spectrum of the  $S_1$  state is then easily obtained by means of standard transient absorption spectroscopy. It is typically dominated by a strong absorption band in the visible region, associated with the transition from the  $S_1$  to a higher excited state, denoted as  $S_n$ . The  $S_1$  state then decays to the ground state with lifetime on the order of units to tens of picoseconds, depending on the conjugation length (Polívka and Sundström 2004).

The behavior of carbonyl carotenoids in polar solvents is, however, markedly different. The spectrum after the relaxation of the  $S_2$  state is more complex, as it may contain an additional redshifted band, which is usually assigned to a transition from the intramolecular charge-transfer (ICT) state (Frank et al. 2000; Zigmantas et al. 2004). The ICT nature and relation to the  $S_1$  state are still a matter of discussion (Zigmantas et al. 2002; Shima et al. 2003; Papagiannakis et al. 2004; Durchan et al. 2012; Wagner et al. 2013; Redeckas et al. 2016). The decay of the  $S_1$  and ICT states in polar solvents is typically faster than that of the  $S_1$  state in the nonpolar solvent. Whether or not these phenomena come to play depends on the structural context of the carbonyl group (part of the lactone ring or the end rings, one or two symmetrically positioned carbonyl groups in the molecule, etc.). In the specific case of a protein-bound carotenoid, one can observe a strong ICT band even for a carbonyl carotenoid having no such band in solution (Šlouf et al. 2012).

Carbonyl carotenoids bound to proteins are typically known for their involvement in energy transfer to (bacterio)chlorophylls ((B)Chls), with efficiencies even approaching unity (Polívka et al. 2006, 2007; Gildenhoff et al. 2010). Carotenoids in OCP have, however, the photoprotective function in the process of NPQ. Currently, there are three models explaining how carotenoids are directly involved in NPQ: (1) energy transfer between the quenched molecule and the carotenoid (Ruban et al. 2007; Staleva et al. 2015), (2) charge transfer between these molecules (Holt et al. 2005) and (3) excitonic interaction between these molecules (Bode et al. 2009). There is no clear evidence for any of these mechanisms in OCP-mediated quenching, and both mechanisms #1 and #2 were suggested to play a role in OCP (Tian et al. 2011; Berera et al. 2013; Polívka et al. 2013).

**Fig. 1** Molecular structures of carotenoids relevant to this study together with their schematic side-view representations. In the schematic representation: *black rectangle* conjugated backbone; *red line*  $\beta 1$  ring; *blue line*  $\beta 2$  ring; *solid line* a conjugated carbonyl on the ring; *dashed line* no conjugated carbonyl on the ring; torsion angles indicated. Carotenoid structures: canthaxanthin (**a**, **b**: *s-cis-s-cis*; **c**, **d**: *s-trans-s-cis*; **e**, **f**: *s-cis-s-trans*; **g**, **h**: *s-trans-s-trans*), echinenone (**m**, **n**: *s-cis-s-cis*), zeaxanthin (**q**, **r**: *s-cis-s-cis*). Schematic structure of carotenoids in solution, shown on canthaxanthin (**i**). Schematic structures of carotenoids in proteins: main form of OCPo-can (**j**, Leverenz et al. 2015), putative configuration in the red form of OCPo-can (**k**), RCP-can (**l**, Leverenz et al. 2015), main form of OCPo-ecN (**o**, Wilson et al. 2010), putative configuration in the red form of OCPo-ecN (**p**)



It has recently been shown that the N-terminal domain of OCP is the active part responsible for quenching, which binds to the phycobilisomes (Leverenz et al. 2014, 2015). It is called the red carotenoid protein (RCP). The C-terminal part is the regulator of the quenching activity (Sutter et al. 2013; Leverenz et al. 2014). Although only OCP is physiologically relevant, absorption and Raman spectra of OCP and RCP shared substantial similarities, demonstrating that the immediate environments of the carotenoids are very similar in both proteins (Leverenz et al. 2014). Thus, information about RCP can help reveal the properties of OCP in vivo. Results of transient absorption

spectroscopy on RCP showed that the carotenoid lifetime is close to that in solution. It was therefore concluded that a part of the carotenoid containing the carbonyl group is exposed to the buffer (Chábera et al. 2011). The recent X-ray structure of RCP, though with a different carotenoid (canthaxanthin) than that studied in Chábera et al. 2011 (3'-hydroxyechinenone), did not confirm a substantial solvent exposure of the carotenoid with the exception of the end rings (Leverenz et al. 2015). Instead, it revealed large differences between the position of the carotenoid in OCP and RCP. This means that upon photoactivation the carotenoid must undergo a substantial translocation—while in

OCPo the two halves of the carotenoid molecule are shared between the two OCP domains, in RCP the carotenoid penetrates deep into the interior of the N-terminal domain, most likely leaving the carotenoid-free C-subunit attached only by the linker (Leverenz et al. 2015). The N-subunit is so activated for the quenching function. This model with detachment of the subunits held together by the linker, forming an elongated structure, was confirmed by a recent study employing various methods including small-angle X-ray scattering (Gupta et al. 2015).

Here, we present a femtosecond time-resolved study of OCP containing various carotenoids (echinenone, canthaxanthin, and zeaxanthin) and of RCP with canthaxanthin. The recently published study (Leverenz et al. 2015) enables us to associate molecular structure with spectroscopic measurements for the OCP–RCP pair with the carotenoid canthaxanthin. Comparisons with OCP binding different carotenoids proved very helpful in addressing the spectral heterogeneity of OCP samples described earlier (Polívka et al. 2013; Kish et al. 2015).

## Materials and methods

### Sample preparation

OCP-Ana-can (OCP from *Anabaena* sp. with the carotenoid canthaxanthin, hereafter called “OCP-can”), OCP-Syn-ecn (OCP from *Synechocystis* PCC6803 with the carotenoid echinenone, hereafter called “OCP-ecn”) and RCP-Syn-can (RCP from *Synechocystis* PCC6803 with the carotenoid canthaxanthin, hereafter called “RCP-can”) were isolated from *E. coli* cells carrying three plasmids containing all the genes necessary for the synthesis of canthaxanthin or echinenone and the *ocp* or *rcp* genes. The production and isolation of these proteins are described in de Carbon et al. (2015) and Leverenz et al. (2015). OCP-Syn-zea (hereafter called “OCP-zea”) was isolated from a *Synechocystis* mutant lacking echinenone and 3'-hydroxyechinenone and overexpressing the *ocp* gene. The construction of the *Synechocystis* mutant and the isolation of OCP-zea are described in Punginelli et al. 2009.

### Spectroscopy

Femtosecond pump–probe measurements were carried out with pulses derived from the modular laser system based on the Spitfire Ace-100F ultrafast Ti–sapphire regenerative amplifier (Spectra Physics) seeded with the Mai Tai SP oscillator (Spectra Physics) and pumped with Empower 30 laser (Spectra Physics). The output from the oscillator consists of pulses with 800-nm central wavelength, ~100-fs pulse width delivered at 1 kHz repetition rate. The

output beam is split into two separate beams. The pump beam is tuned by an optical parametric amplifier (TOPAS, Light Conversion), to reach the desired excitation wavelength (470 and 540 nm for purposes of this study). The excitation intensity of pump pulses was kept below  $2 \times 10^{14}$  photons pulse<sup>-1</sup> cm<sup>-2</sup>. The probe beam is the white-light continuum generated by a 2-mm sapphire plate. The respective polarization between pump and probe pulses is set to the magic angle (54.7°). A detailed description of the experimental setup can be found in Keşan et al. 2016.

All samples were dissolved in 40 mM Tris–HCl buffer with pH 8. The absorbance of all samples was adjusted to ~0.7 OD at 470 nm, which corresponds to <0.2 OD at 540 nm (measured in a 2-mm cuvette). A rectangular 2-mm quartz cuvette with vertical magnetic stirring was used for pump–probe measurements. All measurements were performed at 12 °C using a temperature-controlled cuvette holder (Flash 300, Quantum Northwest).

## Results

### Steady-state absorption spectroscopy

Figure 2 shows steady-state absorption spectra of all studied samples. From the general point of view, OCP-can and OCP-ecn spectra are rather similar. OCP-zea differs in being blueshifted with respect to the other two OCP samples and also exhibits a well-resolved vibrational structure. The RCP-can spectrum is redshifted and has essentially no vibrational structure. The 0–0 bands of OCP-can, OCP-ecn and OCP-zea are at 500, 497 and 493 nm, respectively. For all OCP samples, the 0–0 band is of similar strength as the

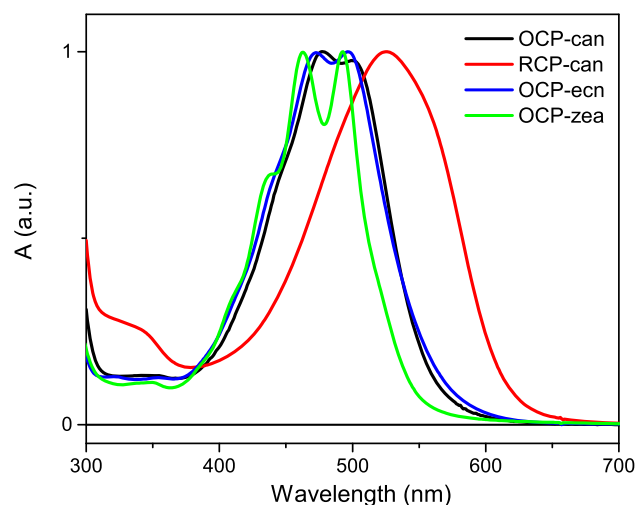


**Fig. 2** Steady-state absorption spectra of studied samples. The spectra are normalized to their maxima

0–1 band that peaks at 477 nm (OCP-can), 472 nm (OCP-ecn) and 463 nm (OCP-zea). This feature is rather unusual for carotenoids because the 0–1 vibrational band is typically the strongest. The increase in the 0–0 band intensity in OCP has been attributed to either OCP<sub>r</sub> partially contributing to the red tail of the carotenoid absorption band (Polívka et al. 2013) or to the presence of more carotenoid configurations in OCP<sub>o</sub> (Kish et al. 2015). To confirm the presence of another band contributing to the red tail of absorption spectra, we deconvoluted the absorption spectra into Gaussian bands (Supporting Information Figs. S1 and S2). The presence of the “red” band was confirmed in all OCP samples; the other bands summed together resulted in the standard carotenoid spectrum with the strongest 0–1 vibrational band, confirming that all the OCP samples exhibit spectral heterogeneity. To study this, the transient measurements on OCP were conducted with two excitation wavelengths, 470 and 540 nm, to address respective sub-populations in the samples.

The maximum of the RCP-can absorption spectrum is largely redshifted to 525 nm. This can point to high polarizability of the protein environment and/or longer effective conjugation length of the carotenoid molecule (Kish et al. 2015). The essentially lost vibrational structure suggests an increased conformational disorder. This heterogeneity is, however, of a different nature than in OCP samples. Presumably, in OCP there exist two well-defined populations of carotenoid molecules (two different carotenoid configurations), resulting in a maintained vibrational structure. In RCP, however, the vibrational structure is lost, which may mean that there exists a distribution of configurations with slightly altered structures, nonetheless, belonging to a single carotenoid configuration. The configurational homogeneity of OCP<sub>r</sub> (whose part containing the carotenoid is RCP) was confirmed by resonance Raman data (Kish et al. 2015).

## Transient absorption spectroscopy

### Transient absorption spectra

Figure 3 shows transient absorption spectra of all studied samples at times best representing the  $S_1$ – $S_n$  signal, with emphasized differences between excitations at 470 and 540 nm. After 540 nm compared to 470-nm excitation of OCP-can (Fig. 3a), there is a slight redshift both in the ground-state bleaching (GSB; 512 vs. 505 nm) and in the excited-state absorption (ESA; 607 vs. 600 nm). The RCP sample differs in many aspects. The GSB is redshifted, broad and unresolved as expected based on the absorption spectrum. The shoulder, seen in OCP-can around 600 nm,

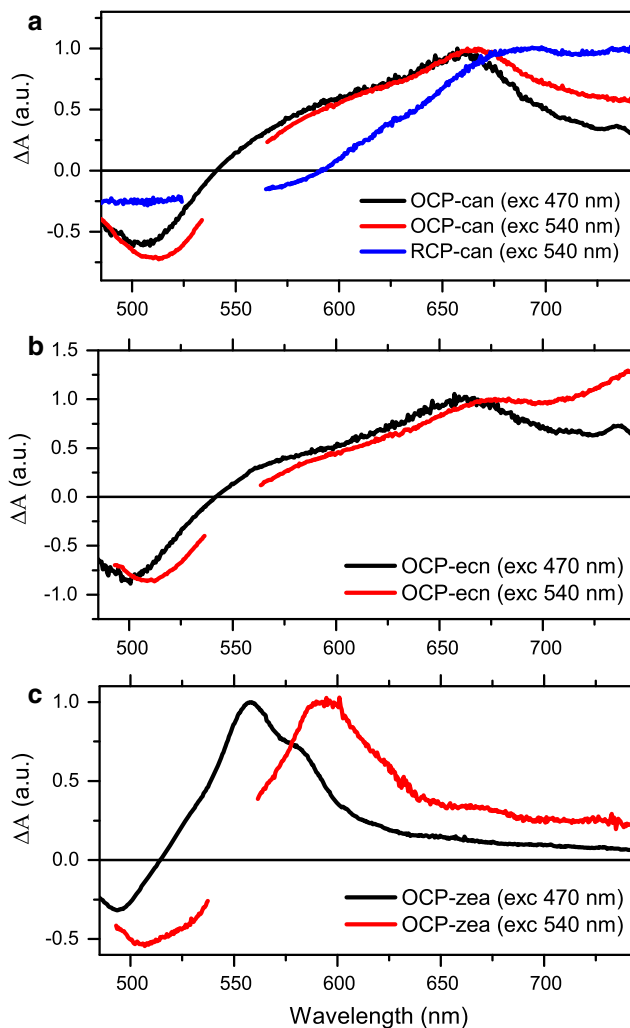


**Fig. 3** Transient absorption spectra normalized to the maximum of the  $S_1$ – $S_n$  transition: **a** OCP-can excited at 470 nm taken at 0.45 ps (black) and 540 nm taken at 0.45 ps (red), RCP-can excited at 540 nm taken at 0.2 ps (blue); **b** OCP-ecn excited at 470 nm taken at 0.3 ps (black) and excited at 540 nm taken at 0.2 ps (red); **c** OCP-zea excited at 470 nm taken at 0.9 ps (black) and 540 nm taken at 0.7 ps (red)

is not present in RCP. The maximum of  $S_1$ – $S_n$  transition is redshifted to  $\sim 685$  nm. Most importantly, another broad and redshifted band is present ( $\sim 740$  nm). Such redshifted bands are indicative of a transition from the ICT state (Berera et al. 2012; Šlouf et al. 2012; Berera et al. 2013). We will denote the  $\sim 740$ -nm band as an “ICT band” in the following text. From this perspective, one can distinguish also the contribution of the ICT signal to the transient spectra of OCP-can whereby the ICT signal contribution is stronger for the 540 than for the 470-nm excitation. More details about the ICT band assignment will be mentioned in Discussion.

Apart from the red-most part of their transient absorption spectra, OCP-ecn (Fig. 3b) data for the two excitations



(470 and 540 nm) exhibit similar differences as OCP-can. The GSB moves from 500 to 510 nm and the  $S_1$ – $S_n$  ESA from 661 to 675 nm. However, the signal around 740 nm is much stronger for the latter excitation, suggesting a strong contribution of the ICT signal.

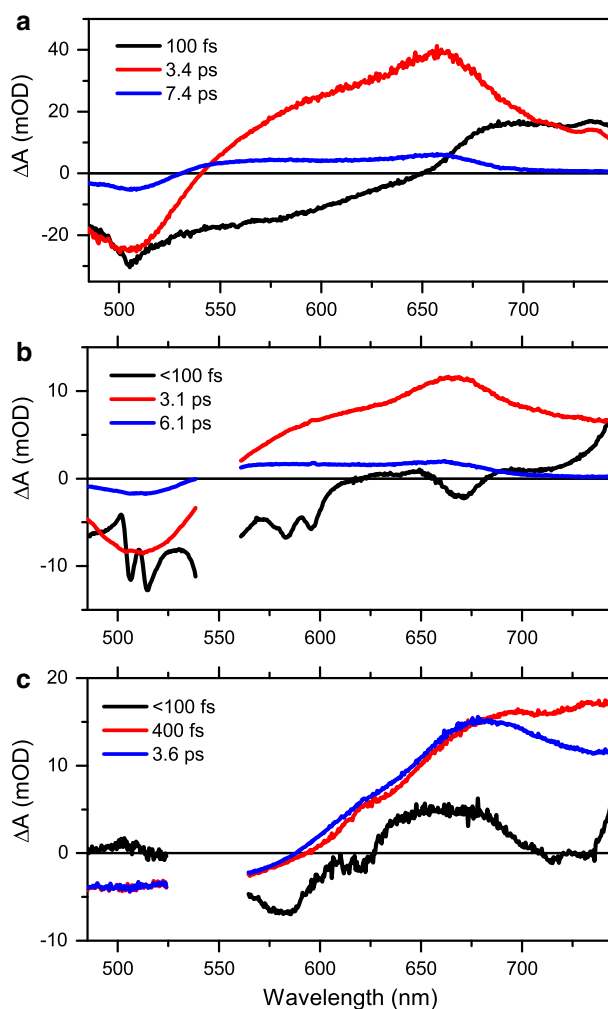
Transient absorption spectra of OCP-zea (Fig. 3c) are qualitatively very different from the others. Generally speaking, this is caused by the fact that zeaxanthin is a non-carbonyl carotenoid. Moreover, significant differences also appear between transient absorption spectra of OCP-zea after the two excitations. The GSB minimum is shifted from 493 nm (470-nm excitation) to 507 nm (540-nm excitation). The  $S_1$ – $S_n$  maximum is shifted even more, from 558 to 594 nm. The  $S_1$ – $S_n$  band after the longer-wavelength excitation is somewhat “cleaner,” but 470-nm excitation generates a transient spectrum containing an additional shoulder on the low-energy slope. These observations point to the fact that while the 540-nm excitation addresses only one subpopulation of OCP, 470 nm excites both subpopulations.

#### Evolution-associated difference spectra

Figure 4 shows evolution-associated difference spectra (EADS), which result from global fitting of transient absorption spectra of OCP-can excited at 470 nm (Fig. 4a) and 540 nm (Fig. 4b). The dynamics are, generally, very similar after both excitations. The black spectrum is associated with the carotenoid  $S_2$  state, but is rather unreliable given that the lifetime is close to the time resolution of our setup. The black EADS is replaced within the duration of the pump pulse by the red EADS. This EADS consists of GSB in the blue-most part and a broad ESA arising from the  $S_1$ – $S_n$  transition of the carotenoid. The red EADS then decays in  $\sim 3$  ps to the blue, rather weak EADS. This EADS may belong to the  $S_1$ – $S_n$  spectrum of some carotenoid subpopulation with a slower ( $\sim 6$ – $7$  ps) decay.

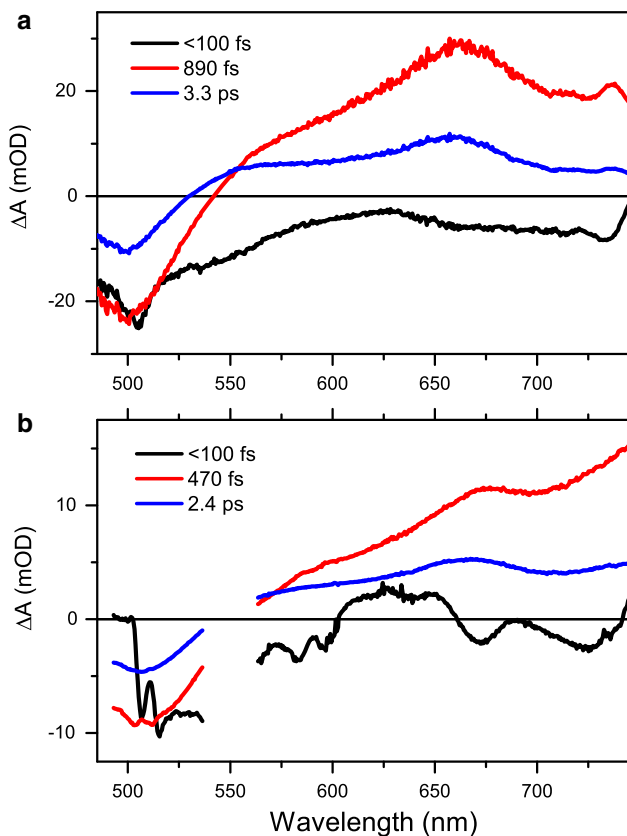
EADS of RCP-can are shown in Fig. 4c. The spectra are obviously rather distinct from those of OCP-can binding the same carotenoid. Most importantly, the red EADS, which appear in less than 100 fs, contain a strong signal redshifted from the  $S_1$ – $S_n$  band. This is the signal from the ICT state. The 0.4-ps time constant is almost exclusively related to the decay of the ICT band. The blue EADS with the lifetime of 3.6 ps then represent mainly the signal associated with the  $S_1$ – $S_n$  transition. Mostly, because of the missing slow component, the overall dynamics of RCP-can is faster than of OCP-can.

Figure 5 shows EADS of OCP-ecn after 470- (Fig. 5a) and 540-nm (Fig. 5b) excitation. Both datasets differ mainly in the reddest part of the spectra. As mentioned above, these differences are ascribed to a stronger ICT signal after 540-nm excitation. As in the case of OCP-can,



**Fig. 4** EADS of OCP-can sample excited at 470 nm (a) and 540 nm (b), RCP-can excited at 540 nm (c)

three time constants were needed to obtain good fits. The first EADS (black) decay faster than the temporal resolution of our setup. The following, red EADS bear signatures of signals from the  $S_1$  and ICT states, the latter being stronger after 540-nm excitation. The ICT signal is associated with a shorter lifetime (0.9 vs. 0.5 ps for 470 and 540 excitation, respectively), which is also confirmed by other studies (Bautista et al. 1999; Frank et al. 2000; Zigmantas et al. 2004). It is remarkable how different the spectral response can be for carotenoids with such similar structures as canthaxanthin and echinenone. The only difference between the two molecules is that canthaxanthin contains carbonyl groups on both end rings, while in echinenone one is missing (Fig. 1m). The last EADS with lifetimes 3.3 ps (470-nm excitation) and 2.4 ps (540-nm excitation) are somewhat stronger than in OCP-can. The overall dynamics of OCP-ecn are faster after 540-nm excitation.



**Fig. 5** EADS of OCP-ecn sample excited at 470 nm (a) and 540 nm (b)

Figure 6 shows EADS of OCP-zea. We will start with the description of EADS resulting from data after 540-nm excitation. They are “cleaner” because just one subensemble of molecules was excited, which is seen both in simpler dynamics with fewer time constants and in higher spectral homogeneity. With the decay of the black EADS appear the red EADS with the lifetime of 1.4 ps. These EADS (red) are spectrally broader than the next one (blue). This finding suggests that the red EADS refer to the transition from the hot  $S_1$  state. This implies that vibrational relaxation of zeaxanthin in OCP-zea is much slower than in solution (Billsten et al. 2005), but a comparable effect was reported earlier for another zeaxanthin-binding protein (Billsten et al. 2003). The blue EADS, thus, corresponds mainly to the  $S_1$ - $S_n$  transition. The  $\sim 7$ -ps  $S_1$  lifetime is shorter compared to the  $\sim 9$ -ps value reported for zeaxanthin in solution (Polívka and Sundström 2004). At the same time, the  $S_1$ - $S_n$  maximum is redshifted to 587 nm. The redshift is in agreement with the shorter lifetime, suggesting that the carotenoid configuration preferentially excited by 540 nm has longer effective conjugation than that in solution. It must be noted, however, that there is another source of redshift in OCP, i.e., the polarizability of the protein environment (Niedzwiędzki et al. 2014).

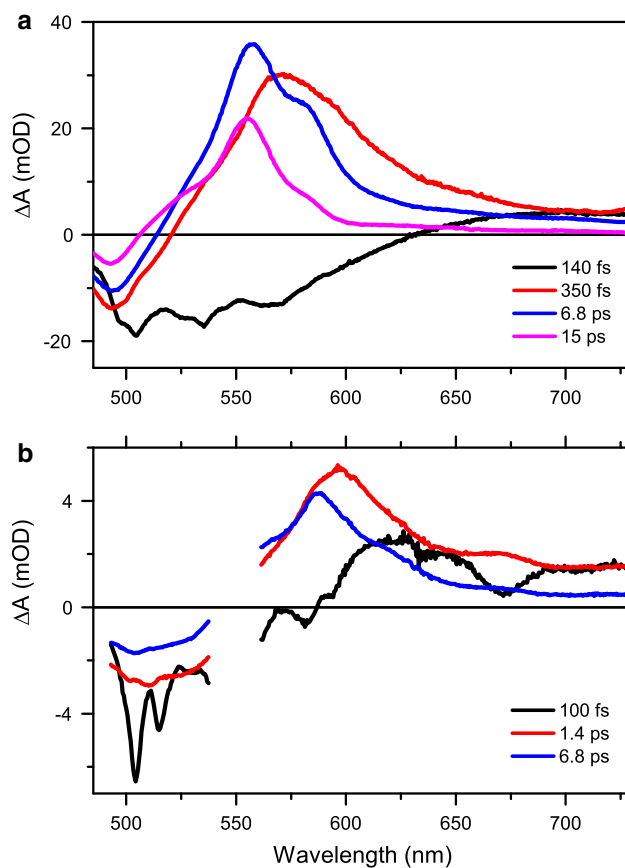


**Fig. 6** EADS of OCP-zea sample excited at 470 nm (a) and 540 nm (b)

The EADS after 470-nm excitation are more complex. To fit the data, four time constants were needed. The red spectrum associated with vibrational relaxation in the  $S_1$  state decays much faster (0.35 ps) than after the 540-nm excitation. The blue spectrum then contains a shoulder on the longer-wavelength slope. Because the next EADS (magenta) differ from the blue one mainly by the absence of this shoulder, the blue EADS can, therefore, be coupled with the decay of that shoulder. Both the spectral position of the shoulder and the lifetime of 6.8 ps correspond with the  $S_1$ - $S_n$  decay after 540-nm excitation (blue EADS in Fig. 6b). Due to this observation, we can confirm that both subpopulations in OCP-zea are excited at 470 nm. The last, magenta EADS corresponds to the signal from the  $S_1$  state of the “blue” subpopulation of OCP-zea, giving the  $S_1$  lifetime of this zeaxanthin  $\sim 15$  ps. Results of the global fitting are summarized in Table 1.

#### Kinetics

Figure 7 supports the statements on the general dynamics mentioned above by showing kinetics at  $S_1$ - $S_n$  maxima for all studied samples and excitation wavelengths. The

**Table 1** Time constants extracted from the global fitting analysis

OCP-can excited at 470 nm	OCP-can excited at 540 nm	RCP-can excited at 540 nm	OCP-ecn excited at 470 nm	OCP-ecn excited at 540 nm	OCP-zea excited at 470 nm	OCP-zea excited at 540 nm
100 fs	<100 fs	<100 fs	<100 fs	<100 fs	140 fs	100 fs
–	–	400 fs	890 fs	470 fs	350 fs	1.4 ps
3.4 ps	3.1 ps	3.6 ps	3.3 ps	2.4 ps	6.8 ps	6.8 ps
7.4 ps	6.1 ps	–	–	–	15 ps	–

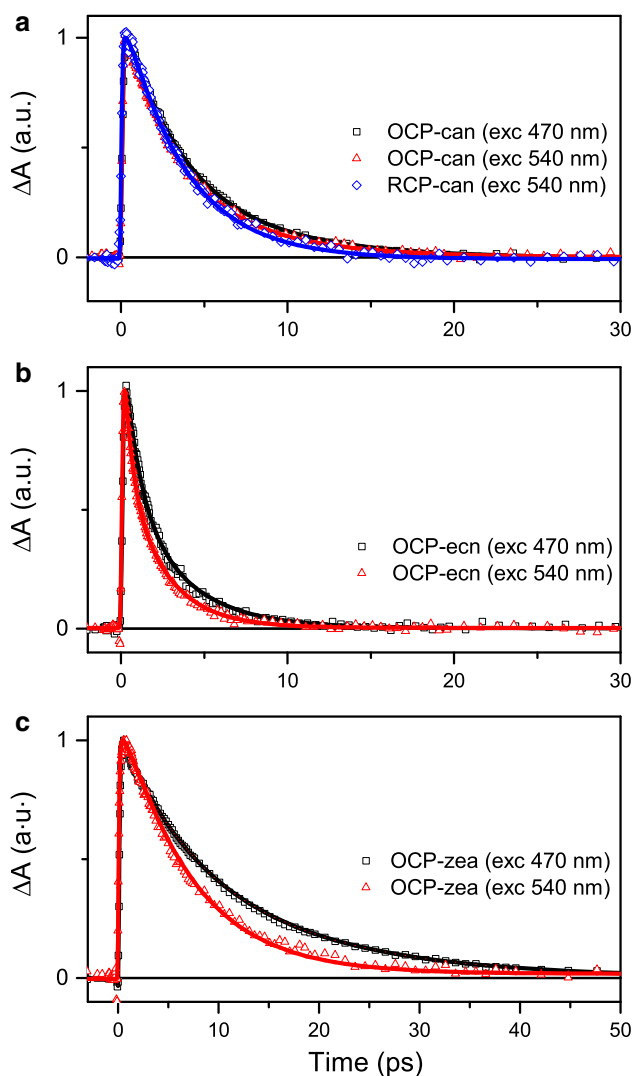


**Fig. 7** Normalized kinetic traces taken at maxima of  $S_1$ – $S_n$  transitions. Solid lines represent the fitted curves. **a** OCP-can excited at 470 nm (probe at 660 nm, black) and 540 nm (at 668 nm, red), RCP-can excited at 540 nm (at 675 nm, blue); **b** OCP-ecn excited at 470 nm (at 660 nm, black) and 540 nm (at 673 nm, red); **c** OCP-zea excited at 470 nm (at 580 nm, black) and 540 nm (at 587 nm, red)

transient spectra of OCP-can for the two excitations are not markedly different (Fig. 3a); so, the dynamics are rather similar (Fig. 7a). The RCP-can dynamics also does not

differ much, but is still faster than that of OCP-can. OCP-ecn transient absorption spectra differ mainly in the reddest part due to the presence of the strong ICT band (Fig. 3b). Consequently, the faster ICT dynamics for the 540-nm excitation results in faster overall dynamics at the  $S_1$ – $S_n$  maximum than for the 470-nm excitation.

OCP-zea exhibits largest differences among the three OCP samples when the kinetics after the two excitations are compared (Fig. 7c). The kinetics after 540-nm excitation are markedly faster than after 470-nm excitation. This observation is in line with the redshifted transient absorption maximum of OCP-zea excited at 540 nm (Fig. 3c), suggesting that a population of zeaxanthin with larger conjugation length is selected by this excitation wavelength.

## Discussion

### What is an ICT signal, and what is not?

In the above text, we state that the ICT band is the red-most signal in the recorded spectra of RCP-can and OCP-ecn after 540-nm excitation (Fig. 3a, b). This, however, contradicts an earlier published work on OCP-hecn (OCP with 3'-hydroxyechinenone), where the  $\sim 660$ -nm band in transient absorption spectra was considered to be the ICT band. Such an assignment was based on the large difference between transient absorption spectra of 3'-hydroxyechinenone in solution and in OCP (Polívka et al. 2005). In this study, however, we were able to extend our measurements more to the near-IR spectral region with the result of recording a strong signal above  $\sim 730$  nm. Consequently, the band at  $\sim 660$  nm is considered as the  $S_1$ – $S_n$  signal here (Fig. 3a, b), but the one above  $\sim 730$  nm is considered as the ICT-related signal (Fig. 3a, b), in agreement with more recent studies (Berera et al. 2012; Šlouf et al. 2012; Berera et al. 2013). To support this statement, one can compare transient spectra of OCP-can (Fig. 3a) with those of canthaxanthin in solution (Chábera et al. 2009). Given the overall symmetry of canthaxanthin, unequivocally unperturbed in solution, no features in the



transient spectra were associated with the ICT signal (Chábera et al. 2009). Based on the similarity of transient spectra/EADS of canthaxanthin in solution with those of OCP-can, we assume the signal at  $\sim 660$  nm (Fig. 3a) is not related to a transition from the ICT but rather from the  $S_1$  state. The same is true for OCP-ecn, where the transient spectra of OCP-ecn excited at 470 nm resemble those of echinenone in solution, where no ICT signal was identified due to the *s-cis* configuration of the ring containing the carbonyl group (Chábera et al. 2009). Therefore, only the signal above  $\sim 730$  nm, clearly observed in OCP-ecn excited at 540 nm (Fig. 3b), is considered here as the ICT signal.

### Spectroscopy–structure relationships in OCP and RCP

Recently published X-ray structures of OCP-Syn-can and RCP-Syn-can (Leverenz et al. 2015) enable the correlation between structural differences of these two pigment proteins and our spectroscopic results. The OCP and RCP proteins studied here contain the carotenoid canthaxanthin with a conjugated carbonyl group, which is known to have dramatic effect on transient absorption spectra through the ICT state (Zigmantas et al. 2004; Enriquez et al. 2010; Šlouf et al. 2012). Whether or not the ICT state-related signal is recorded for a carbonyl carotenoid depends on polarity of the environment and the symmetry of the molecule. Strong ICT signal and  $S_1$  lifetime shortening were obtained in polar solvents (Frank et al. 2000; Zigmantas et al. 2004). However, in case of symmetrically positioned carbonyl groups (e.g., in crocetinindial, canthaxanthin), no ICT-related signal is detected even in a polar solvent (Chábera et al. 2009; Enriquez et al. 2010). On the other hand, a strong ICT signal is recorded if just one of the carbonyls is reduced to a hydroxyl as in 8,8'-diapocarotene-8'-ol-8-al (Enriquez et al. 2010). But even asymmetry of the conjugated carbonyl cannot guarantee the presence of the ICT band in solution as evidenced by echinenone (Chábera et al. 2009). Its single conjugated carbonyl group is located on a terminal ring, which should be twisted in solution by about  $45^\circ$  with respect to the main conjugated chain, as evidenced for other carotenoids with terminal rings (Young et al. 2002; Dreuw 2006; Fuciman et al. 2015). In such an arrangement, the effect of the conjugated carbonyl is apparently too small to induce an ICT signal, confirming that the torsion around the single bond adjacent to the terminal ring (Fig. 1) determines how much the conjugated bonds on the rings contribute to spectroscopic properties (Fuciman et al. 2015). It is thus likely that the ICT activity will be significant for a configuration close to *s-trans* (Fig. 1c, 1e), as proposed earlier (Zigmantas et al. 2004; Šlouf et al. 2012).

Given the symmetric position of carbonyls in canthaxanthin (Fig. 1a), no ICT-related signal might be expected in OCP or RCP. However, the protein can force the molecule into a configuration, which is unstable in solution (Šlouf et al. 2012) as it is the case of canthaxanthin in OCP/RCP (Leverenz et al. 2015, Fig. 1j, l). In both cases, the carotenoid molecule is highly non-symmetric, mainly in terms of the orientation of the end rings with respect to the rest of the conjugated backbone. In OCP, the orientation of both rings is very much of an out-of-plane character, even more than in solution: The  $\beta_1$  ring torsion is  $116^\circ$ , and for  $\beta_2$  it is  $72^\circ$  (Fig. 1j). The respective dihedral angles in RCP are  $64^\circ$  and  $163^\circ$  (Fig. 1l).

Based on above-mentioned information, one can propose the following hypotheses:

1. Given the significant off-plane torsion of the terminal rings in OCP-can, the conjugated bonds at the rings (and thus also the carbonyls) will be virtually isolated from the conjugated backbone (Fig. 1j), leading to weak/no ICT state-related phenomena in transient signal of OCP-can.
2. Because of the loss of symmetry in the position of the carbonyls and the nearly *s-trans* orientation of the  $\beta_2$  ring in RCP-can (Fig. 1l), we expect the ICT state be active and give rise to the typical signal in transient absorption spectra.

It is clear from Fig. 3a that both hypotheses are confirmed. Although there is a nonzero signal in the ICT region in OCP mainly after the 540-nm excitation, the difference between OCP-can and RCP-can is obvious. The OCP structure can even give us a clue why there is some ICT signal recorded in OCP-can. Although the best condition for the ICT to be observed is the *s-trans* position of the carbonyl group, one can imagine a gradually lower ICT activity as the distortion from the *s-trans* configuration becomes larger. At the same time, the position of the two rings is non-symmetric (Fig. 1j). Thus, both conditions for recording the ICT signal are at least partially met in OCP-can leading to a weak ICT signal.

Our data also shed new light on the results obtained for RCP from *A. maxima* (Chábera et al. 2011). In that case, no ICT signal was recorded and the lifetime of RCP-hecn was close to that of 3'-hydroxyechinenone in solution. It was therefore concluded that the part of carotenoid, which resides in the C-terminus of OCP, is exposed to the solvent. However, Leverenz et al. 2015 suggest that there is a significant movement of the carotenoid during the transition from OCPo to OCP<sub>r</sub> (demonstrated on RCP). Therefore, the carotenoid would be embraced by the protein also in RCP. If we assume the configuration of 3'-hydroxyechinenone is similar to that of canthaxanthin in RCP, the lack of the ICT signal is not surprising. The  $\beta_1$  ring, the only

ring containing the conjugated carbonyl in 3'-hydroxyechinenone, is significantly distorted from the *s-trans* configuration (Fig. 11), thereby preventing observation of an ICT state-related signal. Although the  $\beta 2$  ring in configuration close to *s-trans* is crucial for the ICT activity in RCP-can, the same configuration in RCP-hecn does not lead to ICT band observation because the  $\beta 2$  ring does not contain the carbonyl group. The redshift of RCP absorption spectra, explained in Chábera et al. 2011 by aggregation, probably has different reasons. First, RCP with respect to the OCP population excited at 470 nm has longer conjugation mainly because the  $\beta 2$  ring assumes the configuration close to *s-trans*. However, no significant lifetime shortening associated with longer conjugation is observed in either RCP-can, presented here (see Fig. 7a), or RCP-hecn reported earlier (Chábera et al. 2011). Thus, another reason for the redshift may be the same as proposed for the redshift of carotenoids in OCP compared to solution, i.e., an increase in the polarizability of the environment (Niedzwiedzki et al. 2014).

### Heterogeneity of OCP

The data presented here clearly imply that the OCP sample is spectrally heterogeneous. This conclusion follows both from the absorption spectra (Fig. 2 and Supporting Information, Fig. S1 and Fig. S2) as well as differences between transient absorption spectra measured after 470- and 540-nm excitations (Fig. 3). Two hypotheses, attempting to explain this heterogeneity, were proposed. The first assumes, based on spectral deconvolution of absorption spectra, that the red wing of the OCP spectrum corresponds to the activated OCP (OCP<sub>r</sub>), which is supposedly present in the sample exposed to ambient light (Polívka et al. 2013). The second hypothesis relies on results of resonance Raman spectroscopy, showing that even the Raman spectrum of OCP excited at the red edge of absorption spectrum differs from that of the fully activated OCP<sub>r</sub> (Kish et al. 2015). These authors conclude that the red part of the OCP spectrum still arises from the inactive OCP<sub>o</sub> yet with different spectral properties than the main form.

To test these hypotheses, we performed a study on OCP-zea (Fig. 2, green), which does not undergo any light-induced activation (Punginelli et al. 2009). Thus, any sign of spectral heterogeneity cannot be ascribed to the presence of active OCP<sub>r</sub>, but it must be a consequence of heterogeneity of the inactive OCP<sub>o</sub> itself. The steady-state absorption spectrum suggests that some heterogeneity in carotenoid binding is present (Fig. 2) because the 0–1 transition typically dominates the absorption spectrum of zeaxanthin. Yet in OCP-zea the 0–0 and 0–1 transitions are of similar magnitude, indicating the presence of an extra absorption

band at the red edge of absorption spectrum. However, in contrast to OCP-can and OCP-ecn, adding a single redshifted band does not provide good fit of the OCP-zea absorption spectrum. Instead, fitting the OCP-zea spectrum as a sum of two full carotenoid spectra results in a reasonable fit (Supporting Information, Fig. S2).

The heterogeneity of OCP-zea is further confirmed by transient absorption spectroscopy. Two excitation wavelengths were applied: one to select, preferentially, the putative redshifted OCP-zea (540 nm) and the other with stronger contribution of the other form of OCP-zea (470 nm). The results presented in Fig. 3c and global fits in Fig. 6 confirm beyond doubt that the sample is largely heterogeneous. OCP-zea must be able to accommodate carotenoid molecules with two significantly different configurations. The redshift is in agreement with the shorter lifetime, suggesting that the carotenoid configuration excited preferentially by 540 nm has longer effective conjugation than that excited by 470 nm. Interestingly, however, the redshifted zeaxanthin has less resolved vibrational bands (Supporting Information, Fig. S2), suggesting that it is rather loose in its binding site. Thus, we can conclude that the spectral heterogeneity indeed arises from OCP<sub>o</sub> itself and not from an activated OCP<sub>r</sub> superimposed on the spectrum of OCP<sub>o</sub>. We denote the OCP<sub>o</sub> subpopulation excited by 470-nm pulses as the “main form” (based on the larger total contribution to the steady-state spectrum—Supporting Information, Fig. S2) and the subpopulation excited by 540-nm pulses as the “redshifted form.”

Assuming that the crystal structures of OCP (Kerfeld et al. 2003; Leverenz et al. 2015) refer to the main form excited at 470 nm, we can ask what is the carotenoid configuration in the redshifted OCP<sub>o</sub> excited at 540 nm. The main form of OCP<sub>o</sub>-ecn (Fig. 3b) has a rather weak ICT signal. This is a consequence of the partial out-of-plane torsion of the  $\beta 1$  ring containing the carbonyl group with respect to the conjugated backbone, which is 146° (Wilson et al. 2010, Fig. 1o). However, echinenone in the red form of OCP<sub>o</sub>-ecn should have the ring closer to *s-trans* configuration because of the stronger ICT signal (Fig. 3b). Due to the hydrogen bonding of the  $\beta 1$  ring to neighboring amino acids and quite tight packing around the other ring, one can assume that the rings cannot move much. On the other hand, the conjugated chain may have some room to move (Kish et al. 2015). While the  $\beta 1$  ring assumes a configuration close to *s-trans* through ~30° rotation of the conjugated backbone (Fig. 1p), the dihedral angle of the other ring is most probably also affected due to rigidity of the conjugated chain. In the first approximation, one can assume the torsion angle of the  $\beta 2$  ring changes to a similar extent, reaching 80°–90° (Fig. 1p) as compared to the value of 53° in the main form (Fig. 1o).

One can explain the spectroscopic behavior of OCPo-can with the same model. The corresponding  $\beta 1$  ring torsion in the main form is  $116^\circ$  (Fig. 1j). If the chain is turned to the same extent in the red form of OCPo-can, as in OCPo-ecn, the  $\beta 1$  ring assumes the configuration close to that of the main form of OCPo-ecn ( $\sim 150^\circ$ , Fig. 1k). Interestingly, the magnitude of the ICT signal is similar for the red form of OCPo-can and the main form of OCPo-ecn (compare the red curve in Fig. 3a and the black curve in Fig. 3b, respectively). The  $\beta 2$  torsion angle in the red form of OCPo-can then becomes  $\sim 100^\circ$  (Fig. 1k), essentially isolating the  $\beta 2$  ring from conjugation. Within our hypothesis, the overall structure of canthaxanthin in the red form of OCPo-can is still highly non-symmetric, enabling some ICT signal to be recorded, but the  $\beta 1$  ring is still quite far from *s-trans* to enable the signal of similar magnitude as in the red form of OCPo-ecn.

Regarding OCP-zea, there is no structural information available. Due to the absence of the carbonyl oxygen on the ring, one can even expect quite a different configuration because no hydrogen bonds fix the structure as in case of OCP-can and OCP-ecn (Kerfeld et al. 2003; Wilson et al. 2010; Leverenz et al. 2015). In any case, zeaxanthin in the main form of OCP-zea must be locked in a well-defined configuration as resolution of vibrational bands in the absorption spectrum (Fig. S2) is clearly better than for zeaxanthin in solution (Britton et al. 2004). One can, however, estimate the effective conjugation length of zeaxanthin in the main and redshifted form. The  $S_1$  lifetime of the main form is  $\sim 15$  ps, while the corresponding lifetime of the red form amounts to  $\sim 7$  ps (Fig. 6). None of these values match the zeaxanthin  $S_1$  lifetime in solution, which is  $\sim 9$  ps (Polívka and Sundström 2004). However, the zeaxanthin effective conjugation length can be modified in the protein by turning the rings around the neighboring single bonds (Fig. 1q). This carotenoid may, then, theoretically assume configurations with effective conjugation length from 9 (torsion angle of both rings  $90^\circ$ , isolation of rings from conjugation) to 11 (torsion angles  $180^\circ$ , conjugation extended to the rings). The corresponding lifetime interval is from  $\sim 23$  to  $\sim 4$  ps, respectively (Fuciman et al. 2015). Both values obtained from our measurements,  $\sim 15$  and  $\sim 7$  ps, fit into this interval. Based on the analysis in Fuciman et al. 2015, we can estimate the effective conjugation length of the two OCP-zea populations to be  $\sim 9.4$  (main form) and  $\sim 10.4$  (red form).

## Conclusions

Spectroscopic results of this study confirm differences between RCP and OCP, which match those obtained from the recent X-ray structures (Leverenz et al. 2015). The

most important marker discriminating between possible carotenoid configurations in OCP is the presence/absence of the ICT band in transient absorption spectra. However, we do not ascribe the presence of the ICT state any physiological role for the following two reasons: (1) The decay of RCP-can with an active ICT state is not significantly faster than that of OCP-can without the ICT state activity. Moreover, given the  $\sim 3$  orders of magnitude faster excited-state decay of carotenoid  $S_1$  state compared to excited bilin in phycobilisome any carotenoid would serve the purpose with essentially identical efficiency. (2) While RCP-can has an active ICT state, RCP-hecn (Chábera et al. 2011) has not. However, both these RCPs serve as quenchers of phycobilisome fluorescence (Leverenz et al. 2014, 2015). This suggests that the ICT state is not important in the quenching process. We, therefore, propose that the ICT state is a side effect generated as a consequence of the fine-tuning of  $S_1$  energy through ring rotations. The fact that the  $\beta 1$  ring with the carbonyl oxygen is a conserved structural feature in both photoactive RCPs (RCP-can and RCP-ecn) suggests a specific interaction between these carotenoid structures and the phycobilisome, again pointing to the appearance of carbonyl carotenoid-related spectroscopic features as side effects.

Furthermore, an important conclusion is our confirmation that the spectral heterogeneity of OCP, visible even in absorption spectra (Fig. 2, Fig. S1, and Fig. S2), is not the consequence of convoluted OCPo and OCPr absorption spectra. Instead, it appears as a result of two spectral variants of OCPo, denoted here the main and the redshifted form of OCPo. The ultimate evidence provides OCPo-zea, which exhibits clear spectral heterogeneity, though having no photoactivity which would be necessary to form OCPr. Another line of evidence comes through the comparison of transient absorption spectra of the redshifted OCPo with RCP, which are strikingly different (Fig. 3a).

We also hypothesize the possible carotenoid configurations of the redshifted OCPo-can and OCPo-ecn. We adhere to the assumption that the rings are rather immobile and the whole conjugated chain can turn, forming (at least) two configurations, which give rise to the unusual appearance of the OCP steady-state spectrum.

**Acknowledgments** The research in Czech Republic was supported by the Czech Science Foundation grant P501/12/G055. The research in France was supported by the Centre National de la Recherche Scientifique, the Commissariat à l’Energie Atomique, and Phycosource (a CIFRE fellowship to C.B.C.).

## References

Bautista JA, Connors RE, Raju BB et al (1999) Excited state properties of peridinin: observation of a solvent dependence of

- the lowest excited singlet state lifetime and spectral behavior unique among carotenoids. *J Phys Chem B* 103:8751–8758. doi:[10.1021/jp9916135](https://doi.org/10.1021/jp9916135)
- Berera R, van Stokkum IHM, Gwizdala M et al (2012) The photophysics of the orange carotenoid protein, a light-powered molecular switch. *J Phys Chem B* 116:2568–2574. doi:[10.1021/jp2108329](https://doi.org/10.1021/jp2108329)
- Berera R, Gwizdala M, van Stokkum IHM et al (2013) Excited states of the inactive and active forms of the orange carotenoid protein. *J Phys Chem B* 117:9121–9128. doi:[10.1021/jp307420p](https://doi.org/10.1021/jp307420p)
- Billsten HH, Bhosale P, Yemelyanov A et al (2003) Photophysical properties of xanthophylls in carotenoproteins from human retinas. *Photochem Photobiol* 78:138–145. doi:[10.1562/0031-8655\(2003\)0780138PPOXIC2.0.CO2](https://doi.org/10.1562/0031-8655(2003)0780138PPOXIC2.0.CO2)
- Billsten HH, Pan J, Sinha S et al (2005) Excited-state processes in the carotenoid zeaxanthin after excess energy excitation. *J Phys Chem A* 109:6852–6859. doi:[10.1021/jp052227s](https://doi.org/10.1021/jp052227s)
- Bode S, Quentmeier CC, Liao P-N et al (2009) On the regulation of photosynthesis by excitonic interactions between carotenoids and chlorophylls. *Proc Natl Acad Sci U S A* 106:12311–12316. doi:[10.1073/pnas.0903536106](https://doi.org/10.1073/pnas.0903536106)
- Britton G, Liaaen-Jensen S, Pfander H (2004) Carotenoids: handbook. Birkhäuser, Basel
- Chábera P, Fuciman M, Hříbek P, Polívka T (2009) Effect of carotenoid structure on excited-state dynamics of carbonyl carotenoids. *Phys Chem Chem Phys* 11:8795–8803. doi:[10.1039/b909924g](https://doi.org/10.1039/b909924g)
- Chábera P, Durchan M, Shih PM et al (2011) Excited-state properties of the 16 kDa red carotenoid protein from *Arthrospira maxima*. *Biochim Biophys Acta Bioenerg* 1807:30–35. doi:[10.1016/j.bbabi.2010.08.013](https://doi.org/10.1016/j.bbabi.2010.08.013)
- De Carbon CB, Thurotte A, Wilson A et al (2015) Biosynthesis of soluble carotenoid holoproteins in *Escherichia coli*. *Sci Rep* 5:9085. doi:[10.1038/srep09085](https://doi.org/10.1038/srep09085)
- Dreuw A (2006) Influence of geometry relaxation on the energies of the S1 and S2 states of violaxanthin, zeaxanthin, and lutein. *J Phys Chem A* 110:4592–4599. doi:[10.1021/jp057385y](https://doi.org/10.1021/jp057385y)
- Durchan M, Fuciman M, Šlouf V et al (2012) Excited-state dynamics of monomeric and aggregated carotenoid 8'-apo- $\beta$ -carotenal. *J Phys Chem A* 116:12330–12338. doi:[10.1021/jp310140k](https://doi.org/10.1021/jp310140k)
- Enriquez MM, Fuciman M, Lafountain AM et al (2010) The intramolecular charge transfer state in carbonyl-containing polyenes and carotenoids. *J Phys Chem B* 114:12416–12426. doi:[10.1021/jp106113h](https://doi.org/10.1021/jp106113h)
- Frank HA, Bautista JA, Josue J et al (2000) Effect of the solvent environment on the spectroscopic properties and dynamics of the lowest excited states of carotenoids. *J Phys Chem B* 104:4569–4577. doi:[10.1021/jp000079u](https://doi.org/10.1021/jp000079u)
- Fuciman M, Keşan G, LaFountain AM et al (2015) Tuning the spectroscopic properties of aryl carotenoids by slight changes in structure. *J Phys Chem B* 119:1457–1467. doi:[10.1021/jp512354r](https://doi.org/10.1021/jp512354r)
- Gildenhoff N, Amarie S, Gundermann K et al (2010) Oligomerization and pigmentation dependent excitation energy transfer in fucoxanthin-chlorophyll proteins. *Biochim Biophys Acta Bioenerg* 1797:543–549. doi:[10.1016/j.bbabi.2010.01.024](https://doi.org/10.1016/j.bbabi.2010.01.024)
- Gupta S, Guttman M, Leverenz RL et al (2015) Local and global structural drivers for the photoactivation of the orange carotenoid protein. *Proc Natl Acad Sci U S A* 112:E5567–E5574. doi:[10.1073/pnas.1512240112](https://doi.org/10.1073/pnas.1512240112)
- Holt TK, Krogmann DW (1981) A carotenoid-protein from cyanobacteria. *Biochim Biophys Acta Bioenerg* 637:408–414. doi:[10.1016/0005-2728\(81\)90045-1](https://doi.org/10.1016/0005-2728(81)90045-1)
- Holt NE, Zigmantas D, Valkunas L et al (2005) Carotenoid cation formation and the regulation of photosynthetic light harvesting. *Science* 307:433–436. doi:[10.1126/science.1105833](https://doi.org/10.1126/science.1105833)
- Ihalainen JA, D'Haene S, Yermenko N et al (2005) Aggregates of the chlorophyll-binding protein IsiA (CP43') dissipate energy in cyanobacteria. *Biochemistry* 44:10846–10853. doi:[10.1021/bi0510680](https://doi.org/10.1021/bi0510680)
- Kerfeld CA, Sawaya MR, Brahmamdam V et al (2003) The crystal structure of a cyanobacterial water-soluble carotenoid binding protein. *Structure* 11:55–65. doi:[10.1016/S0969-2126\(02\)00936-X](https://doi.org/10.1016/S0969-2126(02)00936-X)
- Keşan G, Litvín R, Bina D et al (2016) Efficient light-harvesting using non-carbonyl carotenoids: energy transfer dynamics in the VCP complex from *Nannochloropsis oceanica*. *Biochim Biophys Acta Bioenerg* 1857:370–379. doi:[10.1016/j.bbabi.2015.12.011](https://doi.org/10.1016/j.bbabi.2015.12.011)
- Kirilovsky D (2007) Photoprotection in cyanobacteria: the orange carotenoid protein (OCP)-related non-photochemical-quenching mechanism. *Photosynth Res* 93:7–16. doi:[10.1007/s11120-007-9168-y](https://doi.org/10.1007/s11120-007-9168-y)
- Kish E, Pinto MMM, Kirilovsky D et al (2015) Echinonone vibrational properties: from solvents to the orange carotenoid protein. *Biochim Biophys Acta Bioenerg* 1847:1044–1054. doi:[10.1016/j.bbabi.2015.05.010](https://doi.org/10.1016/j.bbabi.2015.05.010)
- Leverenz RL, Jallet D, Li M-D et al (2014) Structural and functional modularity of the orange carotenoid protein: distinct roles for the N- and C-terminal domains in cyanobacterial photoprotection. *Plant Cell* 26:426–437. doi:[10.1105/tpc.113.118588](https://doi.org/10.1105/tpc.113.118588)
- Leverenz RL, Sutter M, Wilson A et al (2015) A 12 Å carotenoid translocation in a photoswitch associated with cyanobacterial photoprotection. *Science* 348:1463–1466. doi:[10.1126/science.aaa7234](https://doi.org/10.1126/science.aaa7234)
- Niedzwiedzki DM, Liu H, Blankenship RE (2014) Excited State Properties of 3'-hydroxyechinenone in solvents and in the orange carotenoid protein from *Synechocystis* sp. PCC 6803. *J Phys Chem B* 118:6141–6149. doi:[10.1021/jp5041794](https://doi.org/10.1021/jp5041794)
- Niyogi KK, Truong TB (2013) Evolution of flexible non-photochemical quenching mechanisms that regulate light harvesting in oxygenic photosynthesis. *Curr Opin Plant Biol* 16:307–314. doi:[10.1016/j.pbi.2013.03.011](https://doi.org/10.1016/j.pbi.2013.03.011)
- Papagiannakis E, Larsen DS, van Stokkum IHM et al (2004) Resolving the excited state equilibrium of peridinin in solution. *Biochemistry* 43:15303–15309. doi:[10.1021/bi047977r](https://doi.org/10.1021/bi047977r)
- Polívka T, Sundström V (2004) Ultrafast dynamics of carotenoid excited states—from solution to natural and artificial systems. *Chem Rev* 104:2021–2072. doi:[10.1021/cr020674n](https://doi.org/10.1021/cr020674n)
- Polívka T, Kerfeld CA, Pascher T, Sundström V (2005) Spectroscopic properties of the carotenoid 3'-hydroxyechinenone in the orange carotenoid protein from the cyanobacterium *Arthrospira maxima*. *Biochemistry* 44:3994–4003. doi:[10.1021/bi047473t](https://doi.org/10.1021/bi047473t)
- Polívka T, van Stokkum IHM, Zigmantas D et al (2006) Energy transfer in the major intrinsic light-harvesting complex from *Amphidinium carterae*. *Biochemistry* 45:8516–8526. doi:[10.1021/bi060265b](https://doi.org/10.1021/bi060265b)
- Polívka T, Hiller RG, Frank HA (2007) Spectroscopy of the peridinin-chlorophyll-a protein: insight into light-harvesting strategy of marine algae. *Arch Biochem Biophys* 458:111–120. doi:[10.1016/j.abb.2006.10.006](https://doi.org/10.1016/j.abb.2006.10.006)
- Polívka T, Chábera P, Kerfeld CA (2013) Carotenoid-protein interaction alters the S1 energy of hydroxyechinenone in the Orange Carotenoid Protein. *Biochim Biophys Acta Bioenerg* 1827:248–254. doi:[10.1016/j.bbabi.2012.10.005](https://doi.org/10.1016/j.bbabi.2012.10.005)
- Punginelli C, Wilson A, Routaboul J-M, Kirilovsky D (2009) Influence of zeaxanthin and echinenone binding on the activity of the orange carotenoid protein. *Biochim Biophys Acta Bioenerg* 1787:280–288. doi:[10.1016/j.bbabi.2009.01.011](https://doi.org/10.1016/j.bbabi.2009.01.011)
- Redeckas K, Voiciuk V, Vengris M (2016) Investigation of the S1/ICT equilibrium in fucoxanthin by ultrafast pump-dump-probe and femtosecond stimulated Raman scattering spectroscopy. *Photosynth Res* 128:169–181. doi:[10.1007/s11120-015-0215-9](https://doi.org/10.1007/s11120-015-0215-9)



- Ruban AV, Berera R, Illoaia C et al (2007) Identification of a mechanism of photoprotective energy dissipation in higher plants. *Nature* 450:575–578. doi:[10.1038/nature06262](https://doi.org/10.1038/nature06262)
- Shima S, Ilagan RP, Gillespie N et al (2003) Two-photon and fluorescence spectroscopy and the effect of environment on the photochemical properties of peridinin in solution and in the peridinin-chlorophyll-protein from *amphidinium carterae*. *J Phys Chem A* 107:8052–8066. doi:[10.1021/jp022648z](https://doi.org/10.1021/jp022648z)
- Šlouf V, Chábera P, Olsen JD et al (2012) Photoprotection in a purple phototrophic bacterium mediated by oxygen-dependent alteration of carotenoid excited-state properties. *Proc Natl Acad Sci U S A* 109:8570–8575. doi:[10.1073/pnas.1201413109](https://doi.org/10.1073/pnas.1201413109)
- Staleva H, Komenda J, Shukla MK et al (2015) Mechanism of photoprotection in the cyanobacterial ancestor of plant antenna proteins. *Nat Chem Biol* 11:287–291. doi:[10.1038/nchembio.1755](https://doi.org/10.1038/nchembio.1755)
- Sutter M, Wilson A, Leverenz RL et al (2013) Crystal structure of the FRP and identification of the active site for modulation of OCP-mediated photoprotection in cyanobacteria. *Proc Natl Acad Sci U S A* 110:10022–10027. doi:[10.1073/pnas.1303673110](https://doi.org/10.1073/pnas.1303673110)
- Tian L, van Stokkum IHM, Koehorst RBM et al (2011) Site, rate, and mechanism of photoprotective quenching in cyanobacteria. *J Am Chem Soc* 133:18304–18311. doi:[10.1021/ja206414m](https://doi.org/10.1021/ja206414m)
- Wagner NL, Greco JA, Enriquez MM et al (2013) The nature of the intramolecular charge transfer state in peridinin. *Biophys J* 104:1314–1325. doi:[10.1016/j.bpj.2013.01.045](https://doi.org/10.1016/j.bpj.2013.01.045)
- Wilson A, Ajlani G, Verbavatz J et al (2006) A soluble carotenoid protein involved in phycobilisome-related energy dissipation in cyanobacteria. *Plant Cell* 18:992–1007. doi:[10.1105/tpc.105.040121.1981](https://doi.org/10.1105/tpc.105.040121.1981)
- Wilson A, Punginelli C, Gall A et al (2008) A photoactive carotenoid protein acting as light intensity sensor. *Proc Natl Acad Sci U S A* 105:12075–12080. doi:[10.1073/pnas.0804636105](https://doi.org/10.1073/pnas.0804636105)
- Wilson A, Kinney JN, Zwart PH et al (2010) Structural determinants underlying photoprotection in the photoactive orange carotenoid protein of cyanobacteria. *J Biol Chem* 285:18364–18375. doi:[10.1074/jbc.M110.115709](https://doi.org/10.1074/jbc.M110.115709)
- Wilson A, Punginelli C, Couturier M et al (2011) Essential role of two tyrosines and two tryptophans on the photoprotection activity of the orange carotenoid protein. *Biochim Biophys Acta Bioenerg* 1807:293–301. doi:[10.1016/j.bbabi.2010.12.009](https://doi.org/10.1016/j.bbabi.2010.12.009)
- Yeremenko N, Kouřil R, Ihalainen JA et al (2004) Supramolecular organization and dual function of the IsiA chlorophyll-binding protein in cyanobacteria. *Biochemistry* 43:10308–10313. doi:[10.1021/bi048772i](https://doi.org/10.1021/bi048772i)
- Young AJ, Phillip DM, Hashimoto H (2002) Ring-to-chain conformation may be a determining factor in the ability of xanthophylls to bind to the bulk light-harvesting complex of plants. *J Mol Struct* 642:137–145. doi:[10.1016/S0022-2860\(02\)00444-1](https://doi.org/10.1016/S0022-2860(02)00444-1)
- Zigmantas D, Hiller RG, Sundström V, Polívka T (2002) Carotenoid to chlorophyll energy transfer in the peridinin-chlorophyll-a-protein complex involves an intramolecular charge transfer state. *Proc Natl Acad Sci U S A* 99:16760–16765. doi:[10.1073/pnas.262537599](https://doi.org/10.1073/pnas.262537599)
- Zigmantas D, Hiller RG, Sharples FP et al (2004) Effect of a conjugated carbonyl group on the photophysical properties of carotenoids. *Phys Chem Chem Phys* 6:3009–3016. doi:[10.1039/b315786e](https://doi.org/10.1039/b315786e)